



Phosphate adsorption from home industry laundry wastewater in Indonesia using teak wood-based activated carbon

Gendy Ayodya Alfarizi¹, Noven Pramitasari^{1,*} and Ririn Endah Badriani¹

¹Department of Environmental Engineering, Faculty of Engineering, University of Jember, Kalimantan Street 37, 68121 Jember, East Java, Indonesia

*Corresponding author: novenpramitasari@unej.ac.id

Received 2 June 2025
Revised 28 August 2025
Accepted 7 November 2025

Abstract

Laundry activities significantly contribute to water pollution due to the high phosphate content in detergents. When released into the environment, phosphates can cause eutrophication in aquatic ecosystems. This study evaluates the potential of teak wood dust (*Tectona grandis*) as a low-cost and sustainable precursor for producing activated carbon to reduce phosphate levels in laundry wastewater. Activated carbon was prepared through chemical activation with H_3PO_4 , which enhances porosity, surface area, and form oxygen-containing functional groups that promote phosphate adsorption. The produced activated carbon was characterized by determining its moisture content, ash content, and Fourier Transform Infrared (FTIR) spectrum to identify functional groups. The adsorption was performed in batch mode with variations in adsorbent mass (1, 3, and 5 g) and contact time (90-180 min). The objectives were to assess the effectiveness of teak wood dust-based activated carbon, determine the optimal conditions, and analyze adsorption kinetics. Results showed that teak wood dust-derived activated carbon effectively reduced phosphate concentrations below the standard limit. The highest adsorption efficiency occurred with 5 g of adsorbent and a 90-min contact time, while longer times decreased efficiency. The adsorption followed a zero-order kinetic model ($R^2 = 0.965$), indicating a nearly constant rate. These findings demonstrate that teak wood dust-based activated carbon provides an efficient, eco-friendly, and sustainable solution for treating phosphate-rich laundry wastewater.

Keywords: adsorbent, detergent, efficiency, phosphate level

1. Introduction

The people of Indonesia have long utilized wood, a source of biomass from forests. However, over time, wood utilization has caused environmental problems, as sawdust waste is often piled up, dumped into river, or burned. According to data from the Central Statistics Agency in 2018, teak wood production in East Java reached 183,729.14 m³. Sawdust waste in Indonesia amounts to approximately 0.78 million m³ per year [1]. Sawdust, as a lignocellulosic waste rich in cellulose, hemicellulose, and lignin, is an ideal material for adsorbents in adsorption processes, an effective method for treating phosphate-contaminated wastewater. Activated carbon produced through chemical activation using Potassium hydroxide preparation (KOH) has a porous structure and high surface area, which can significantly increase the adsorption capacity of phosphate ions. Thanks to its high carbon content, including from teak wood, it is a cheap, abundant, and sustainable raw material for producing activated carbon that is effective in wastewater filtration and removal of eutrophication-causing phosphates [2]. As an adsorbent for wastewater treatment, activated carbon is produced through carbonization and an activation process, which can be carried out physically or chemically. Chemical activation typically involves impregnating the carbon material with activating agents. In wastewater treatment, activated carbon is crucial in removing color, odor, and pollutants, including phosphates, from laundry industry effluents [3]. The average phosphate concentration in laundry wastewater is reported to be 4.54 mg/L [4].

Meanwhile, the Regulation of the Minister of Environment of the Republic of Indonesia Number 5 of 2014 sets the maximum permissible phosphate level in wastewater at 2 mg/L. Laundry wastewater contains detergents that present environmental risks, such as the formation of a surface film that obstructs oxygen transfer and poses potential health hazards to humans. Additionally, combining polyphosphates and surfactants in detergents results in elevated phosphate concentrations in water, which contributes to eutrophication. This process promotes excessive algal growth, diminishes dissolved oxygen levels, and ultimately leads to the mortality of aquatic life [5].

2. Methods

2.1 Material

The materials used in this study include distilled water, phosphoric acid (H_3PO_4 , p.a, Merck), sulfuric acid (H_2SO_4 , p.a, Merck), ammonium molybdate ($(NH_4)_2MoO_4$, p.a, MaxLab), ascorbic acid ($C_6H_8O_6$, p.a, Merck), potassium antimony tartrate (p.a, MaxLab), anhydrous potassium dihydrogen phosphate (KH_2PO_4 , p.a., Merck), laundry waste samples, and teak sawdust.

2.2 Adsorbent Preparation

The adsorbent manufacturing process was initiated by drying teak wood sawdust. The material was carbonized in a furnace at 500°C for 2 h after it had been dried. The resulting charcoal was sieved to a 100-mesh particle size and activated by being soaked in a 2 M H_3PO_4 solution for 24 h. After activation, the adsorbent was rinsed with distilled water until the pH was brought to a neutral level and dried using an oven at 90°C [6]. Before being used as an adsorbent, the activated carbon was required to meet the quality standards set by SNI 06-3730-1995 concerning technical activated carbon. To evaluate their quality, moisture and ash content tests were conducted on activated and unactivated carbon samples. According to SNI 06-3730-1995, the moisture content was determined by heating 1 g of the adsorbent sample at 115°C for 3 h to evaporate the water. The weight difference before and after heating was used to calculate the moisture content. To measure ash content, 2 g of the sample were heated at 900°C for 2 h in a furnace. After cooling, the remaining ash was weighed to determine the percentage of ash content.

2.3 Analysis Method

An adsorption analysis method with a batch system was used in this study. The adsorption process was conducted by varying the contact time (90, 120, 150, and 180 min) and the adsorbent mass (1, 3, and 5 g), while a constant stirring speed of 100 rpm was maintained. The aim was to evaluate how the adsorbent mass and contact time affected phosphate removal. Multiple linear regression analysis was applied to determine the relationship and influence of these two variables. The adsorption kinetics were also evaluated using three kinetic models: zero-order, first-order, and second-order models.

2.4 Phosphate Testing

The calibration curve was illustrated as a graph showing the linear relationship between the concentration of the working solution and its absorbance value. A linear regression equation (Equation 1) was derived from the resulting straight line, allowing the phosphate concentration (x) to be determined by substituting the absorbance value (y).

$$y = ax + b \quad (1)$$

Based on the procedure for testing phosphate levels in laundry wastewater outlined in SNI 06-6989.31-2005: Water and Wastewater – Part 31: Method for Testing Phosphate Levels (PO_4^{3-}) by Spectrophotometry, a calibration curve was prepared using phosphate standard solutions with concentrations of 0.0 mg/L, 0.2 mg/L, 0.4 mg/L, 0.8 mg/L, and 1.0 mg/L. The absorbance of these solutions was measured using a UV-Vis spectrophotometer at a wavelength of 880 nm. The absorbance measurements were performed at 10 to 30-minute intervals, and the results were recorded accordingly.

2.5 Adsorption Process

In this study, an adsorption analysis method was employed using a batch system. Adsorption was defined as a physicochemical process in which molecules of a substance (adsorbate), in this case, phosphate, adhered to the surface of a solid material (adsorbent), such as activated carbon from teak wood dust. This process was

differentiated from absorption, where substances penetrated into the bulk of the material. Adsorption is commonly used in wastewater treatment due to its high efficiency in pollutant removal from solutions. The adsorption process was conducted by varying the contact time (90, 120, 150, and 180 min) and the adsorbent mass (1, 3, and 5 g) while maintaining a stirring speed of 100 rpm. The aim was to evaluate how adsorbent mass and contact time influenced phosphate removal efficiency. To analyze the effect of these variables, a two-way Analysis of Variance (ANOVA) test was applied. This statistical test allowed for the determination of whether each independent variable (adsorbent mass and contact time) significantly affected phosphate adsorption efficiency and whether an interaction existed between them. To further understand adsorption behavior, kinetics were analyzed using zero-order, first-order, and second-order kinetic models.

3. Results and discussion

3.1 Characteristics of teak wood powder adsorbent

The quality of activated carbon was evaluated based on the SNI 06-3730-1995 standard, which includes testing for moisture and ash content. These parameters were measured for raw activated charcoal and chemically activated carbon using H_3PO_4 . Fourier Transform Infrared (FTIR) spectroscopy was employed to determine the functional groups contained in activated carbon [7]. FTIR provides infrared spectra that show absorption patterns, helping to identify the compounds or functional groups in the tested samples [8]. The characteristics of the adsorbents derived from teak wood powder were presented in Table 1.

Table 1 Characteristics of teak wood powder adsorbent.

Parameter	Information	Rate (%)	Quality Standards based on SNI 06-370-1995 (%)
Water content	Not Activated	2.35	Max. 15%
	Activated	1.75	
Ash Content	Not Activated	38.13	Max. 10%
	Activated	7.14	

3.1.1 Analysis of water and ash content

According to SNI 06-3730-1995, the maximum allowable moisture content in activated carbon is 15%. In this study, the moisture content of teak wood powder charcoal in the unactivated adsorbent was 2.35%, while in the H_3PO_4 -activated adsorbent, it was 1.75%. As shown in Table 1, the moisture content of the activated carbon meets the quality standard, as it falls well below the maximum limit. The heating process facilitates the evaporation of volatile compounds. Heating using electromagnetic waves accelerates this evaporation and increases the pore size of the carbon material [9]. Enlarging the pore size enhances the surface area for adsorption, thereby improving the adsorbent's overall capacity. The chemical activator (phosphoric acid) also functions as a dehydrating agent, aiding the removal of water and enhancing the efficiency of the adsorption process. A lower moisture content improves the stability and adsorption performance of the material, as excess water can hinder the formation of bonds between the adsorbent and target pollutants [10].

Regarding ash content, SNI 06-3730-1995 sets a maximum limit of 10%. In this study, the ash content of the unactivated adsorbent was 38.13%, whereas the ash content of the H_3PO_4 -activated adsorbent was significantly lower, at 7.14%. As indicated in Table 1, activation successfully reduced ash content, bringing it within the acceptable range. The chemical activation process effectively develops an optimal microporous structure, which increases the specific surface area and enhances adsorption capacity, leading to this reduction. The decrease in ash content is mainly due to the ability of phosphoric acid to dissolve inorganic compounds and minerals present in the raw material during activation, resulting in a purer carbon structure.

Additionally, phosphoric acid helps break down complex molecules and remove unstable impurities, further improving the activation process. The process leads to the formation of a cleaner pore structure, which contributes to more efficient pollutant adsorption. A lower ash content corresponds to higher adsorption potential, particularly for hazardous substances such as heavy metals and organic compounds in wastewater [10].

3.1.2 FTIR test results

FTIR Spectroscopy identifies functional groups in compounds based on infrared absorption frequencies associated with molecular vibrations [11].

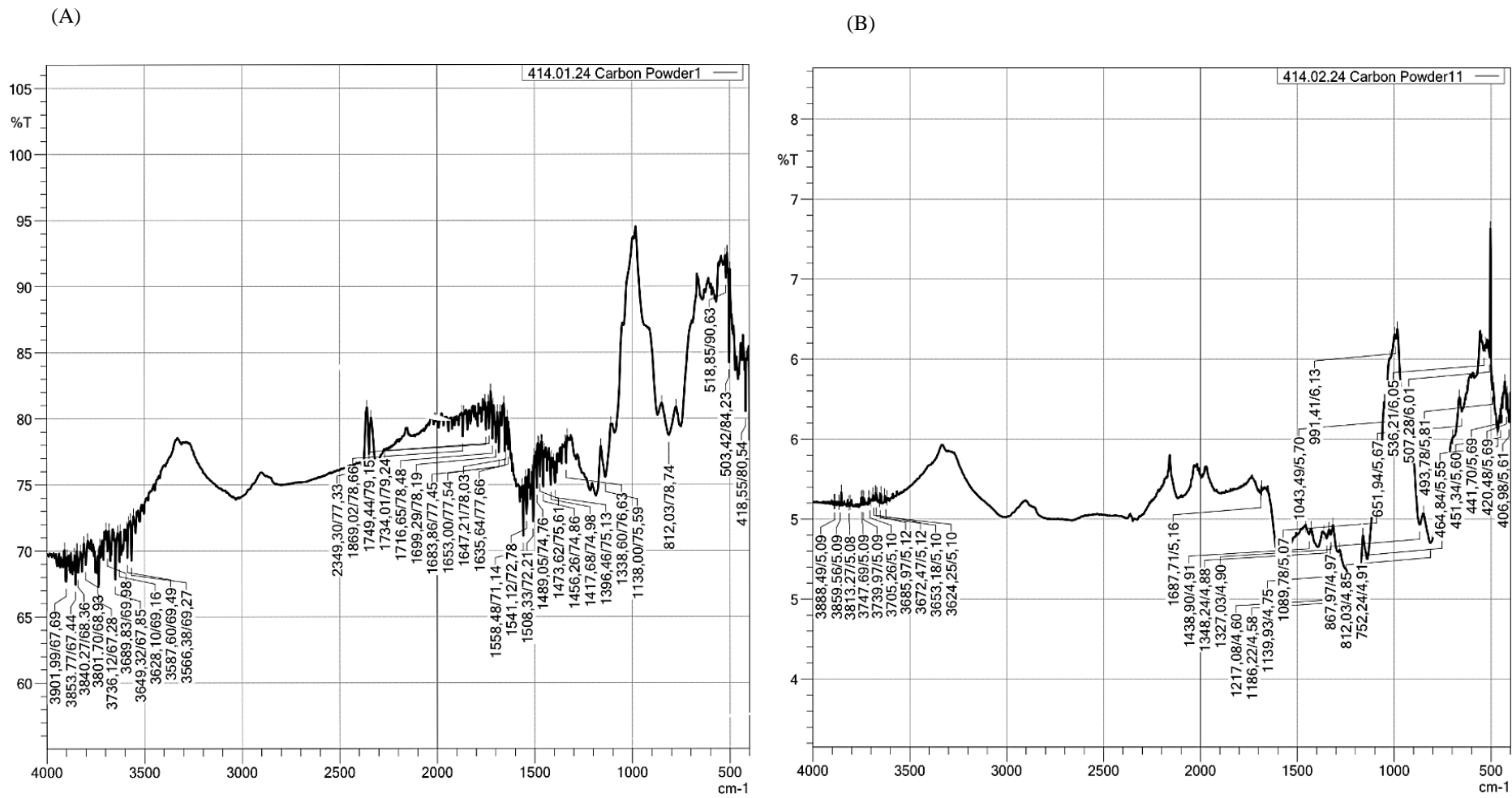


Figure 1 (A) FTIR Results of Unactivated H_3PO_4 and (B) FTIR Results of Activated H_3PO_4 .

The resulting infrared spectrum is a graph that illustrates the relationship between energy intensity and either wavelength (μm) or wavenumber (cm^{-1}) [12]. The FTIR spectra of the unactivated and H_3PO_4 -activated adsorbents are presented in Figures 1 (A) and (B).

Figure 1 shows the FTIR spectrum of the unactivated adsorbent, revealing the presence of hydroxyl (O–H) groups at wavenumber 3901.99 cm^{-1} and 3587.6 cm^{-1} , which indicate bound water or organic compounds. The prominent absorption peaks at 1869.02 cm^{-1} and 1749.44 cm^{-1} correspond to carbonyl (C=O) groups, likely originating from ketones, esters, or carboxylic acids. The peak at 1699.29 cm^{-1} indicates the presence of aromatic C=C double bonds, while the bending vibration observed at 1653 cm^{-1} suggests the presence of Si–O–Si bonds. We attribute the peak at 1473.62 cm^{-1} to asymmetric C–H stretching in aliphatic hydrocarbons. The C–O stretching vibration appears at 1138 cm^{-1} , and the bands at 812.03 cm^{-1} correspond to OSi–O and OAl–O vibrations, indicating silicate and aluminate structures. Significant changes were observed in the FTIR spectrum of the H_3PO_4 -activated adsorbent, as shown in Figure 2. The O–H absorption band shifted from 3901.99 cm^{-1} to 3888.49 cm^{-1} , indicating dehydration. The carbonyl (C=O) group peak at 1869.02 cm^{-1} disappeared, suggesting decarboxylation. The aromatic C=C band shifted from 1699.29 cm^{-1} to 1687.71 cm^{-1} , reflecting alterations in the carbon structure. The intensity of the Si–O–Si vibration at 1653 cm^{-1} decreased, indicating modification of the silica component. The asymmetric C–H stretching band shifted from 1473.62 cm^{-1} to 1438.90 cm^{-1} , while the C–O band shifted from 1138 cm^{-1} to 1217.08 cm^{-1} , indicating changes in the hydrocarbon chain structure. The OSi–O and OAl–O bands initially observed at 812.03 cm^{-1} shifted to 651.94 cm^{-1} or weakened, suggesting changes in the mineral composition and structure of the material.

Table 2 Interpretation of FTIR spectra.

Not Activated	Activated	Functional Group	Wavenumber (cm^{-1})	Reference
3901.99	3888.49	O – H	3065.02 – 4473.12	[27]
3587.6	–	O – H stretching bond	3600 – 3200	[28]
1869.02	–	C = O	2300 – 1800	[12]
1749.44	1687.71	C=O Aromatic combination of Aldehydes, Ketones, Carboxylic Acids, Esters	2000 – 1660	[29]
1699.29	1687.71	C = C Aromatic	1700 – 1400	[12]
1653	–	Si – OH bending vibration	1680 – 1620	[28]
1473.62	1438.90	C-H Asymmetric bond	1475 – 1300	[29]
1138	1217.08	C – O	1300-800	[30]
		– OSi – O	1250 – 950	[28]
		– OAl – O		
812.03	812.03	Symmetrical stretching vibration OSIO/OSIO	820 – 650	[28]
518.85	651.94	C-H Aromatic	700 – 400	[30]

Based on the functional group data of the H_3PO_4 -activated carbon in Table 2, several absorption bands are no longer detected, indicating the loss of specific functional groups. The absorption band at 3587.6 cm^{-1} corresponds to the O–H stretching bond, the absorption at 1869.02 cm^{-1} associated with the carbonyl (C=O) group, and the absorption band at 1653 cm^{-1} related to the Si–OH bending vibration have all disappeared. Additionally, activation with H_3PO_4 plays a key role in removing water molecules, which induces changes in the biopolymer structure, transforming it from aliphatic to aromatic forms. This transformation increases both the carbon stability and the adsorption capacity. Increased mass transfer and the removal of volatile compounds enhance the adsorption capacity by significantly opening more pores on the activated carbon surface [7]. High-temperature heating during the activation process causes the thermal decomposition of specific functional groups such as hydroxyl (-OH), carbonyl (C=O), and carboxyl (-COOH). This activation process also contributes to increased porosity and the formation of a graphite-like structure in the carbon, reducing the number of oxygen-containing functional groups on the surface.

According to Table 2, the peaks corresponding to the absorption bands of the activated H₃PO₄ also show significant changes. The observed changes in the FTIR absorption peaks can be attributed to modifications in the chemical structure and the functional groups that are present within the activated carbon. These alterations reflect the transformation of the surface characteristics and the nature of the bonding, which significantly influence the material's adsorption properties and overall functionality [13]. The shift to a higher wavelength (or a higher wavenumber) indicates an increase in bond energy, likely due to interactions with newly formed functional groups or changes in the chemical environment. Conversely, a shift to lower wavelengths suggests a bond weakening, which could be due to interactions with phosphate molecules or other compounds adsorbed onto the activated carbon surface. These shifts may also reflect hydroxyl, carbonyl, or aromatic bond group changes during the activation and adsorption processes [13].

The H₃PO₄-activated adsorbents exhibit a smaller transmittance percentage range in the FTIR spectrum compared to the unactivated H₃PO₄ adsorbents. Increased porosity and modifications in the chemical structure of the activated carbon during the activation process led to the removal of volatile compounds and create greater regularity in the carbon structure. As a result, there is a decrease in the intensity of infrared absorption by certain functional groups [14]. FTIR analysis shows a significant increase in oxygen-containing functional groups on the surface of the activated carbon, as evidenced by the enhanced intensity of the bands in the spectrum. The successful modification of the activated carbon improves its hydrophilic properties and enhances its adsorption capacity for metal ions or molecules [15].

3.2 Phosphate levels in the adsorption process

Researchers examined the effect of adsorbent mass on phosphate removal by varying the mass to 1, 3, and 5 g, with contact times of 90, 120, 150, and 180 min. The final phosphate concentration was determined using linear regression from the calibration curve. Phosphate levels were calculated based on the absorbance values obtained from a UV-Vis spectrophotometer following the adsorption process. Table 3 shows the results.

Table 3 Final concentration of phosphate.

Adsorbent Mass (g)	Time Variation (min)	Initial Level (mg/L)	Final Concentration (mg/L)	Quality Standard (mg/L)
1	90	6.154	1.913	
	120		1.896	
	150		1.832	
	180		1.252	
3	90	6.154	1.328	
	120		1.256	2
	150		1.226	
	180		1.053	
5	90	6.154	0.786	
	120		1.057	
	150		1.358	
	180		1.459	

Regulation of the Minister of Environment Number 5 of 2014

Based on Table 3, the highest final phosphate removal was observed at an adsorbent mass of 5 g with a contact time of 180 min, which resulted in a phosphate concentration of 1.459 mg/L. A larger adsorbent mass can lead to a decrease in adsorption capacity due to saturation. In the initial phase of the adsorption process, many active sites on the adsorbent surface are available to capture adsorbate molecules. However, as the adsorbent mass increases, the number of filled sites also rises, eventually reaching saturation. Beyond a certain point, increasing the adsorbent mass no longer increases adsorption capacity as most active sites become occupied [16]. An adsorbent

mass of 5 g and a contact time of 90 min achieved the lowest final phosphate concentration of 0.756 mg/L. This finding suggests that multiple factors influence the optimal adsorbent mass and contact time in the phosphate adsorption process using activated carbon. The optimal mass ensures the availability of sufficient active sites to capture phosphate ions, while the appropriate contact time allows the system to reach equilibrium in the adsorption process. The optimal contact time corresponds to a certain duration where the adsorption efficiency reaches its peak, after which re-desorption may occur if the contact time is too long. Thus, in this study, an adsorbent mass of 5 g with a contact time of 90 min proved to be the best condition for phosphate removal [17].

3.3 Phosphate removal efficiency

Phosphate removal is a key parameter evaluated in this study, particularly to assess the effectiveness of the adsorption process. Phosphate levels were measured using a UV-Vis spectrophotometer to ensure the accuracy of the obtained results. Before the adsorption process, wastewater samples from laundry activities had an initial phosphate concentration of 6.154 mg/L.

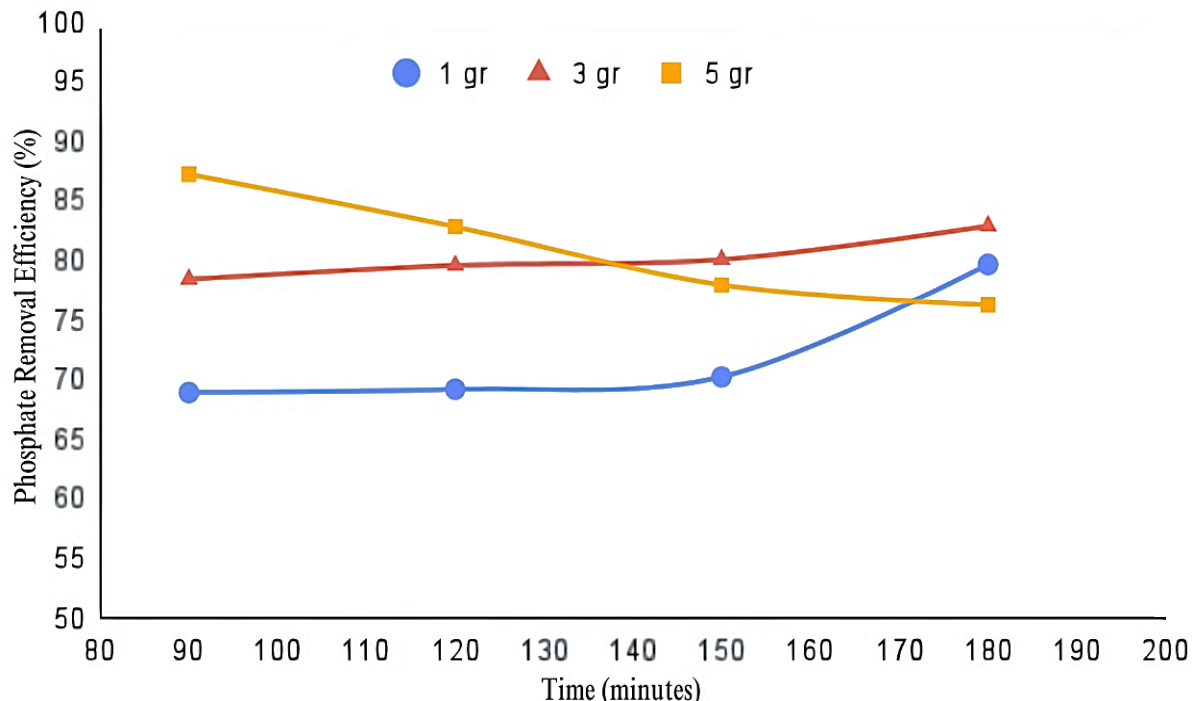


Figure 2 Phosphate removal efficiency.

Based on Figure 2, when compared to adsorbent masses of 1 and 3 g, the adsorbent mass of 5 g exhibited the highest efficiency, reaching 87.23%. A larger adsorbent mass increases the surface area, making it more effective in removing larger quantities of dissolved substances. At an adsorbent mass of 5 g, the increased surface area leads to a higher phosphate adsorption capacity. However, the removal process's effectiveness largely depends on the characteristics of the pores formed during the carbon activation process. Factors such as activation temperature, heating duration, and the nature of the raw materials play crucial roles in determining the number and size of these pores [18]. Increasing the amount of adsorbent can increase the adsorbate absorption ability. This increase occurs due to the increase in surface area available for the adsorption process and the increase in the number of active sites on the adsorbent, along with the increase in the dose used [6].

If the activation temperature is too high, pore blockage may occur due to changes in the carbon structure, which can ultimately reduce adsorption efficiency [19]. Figure 4 also shows that adsorbents with masses of 1 and 3 g experienced an increase in removal efficiency over time. However, at an adsorbent mass of 5 g, the efficiency decreased after 90 min because the adsorbent capacity reached saturation, reducing the removal efficiency. This finding indicates that using larger amounts of adsorbent can enhance adsorption effectiveness, but its long-term performance may decline as the adsorbent surface becomes saturated. Desorption or adsorption saturation reduces the adsorption capacity and removal efficiency over time, which decreases phosphate removal efficiency [4].

3.4 pH value in adsorption process

In addition to phosphate levels, research on pH value is another crucial parameter observed, particularly to monitor changes occurring during adsorption. The pH value was measured using a pH meter to ensure the accuracy of the results. Before adsorption, the laundry wastewater sample had an initial pH of 9.7. This value is still above the permissible range set by the Wastewater Quality Standards, as outlined in PerMen LHK Number 5 of 2014, which specifies that the allowable pH value should fall between 6 and 9.

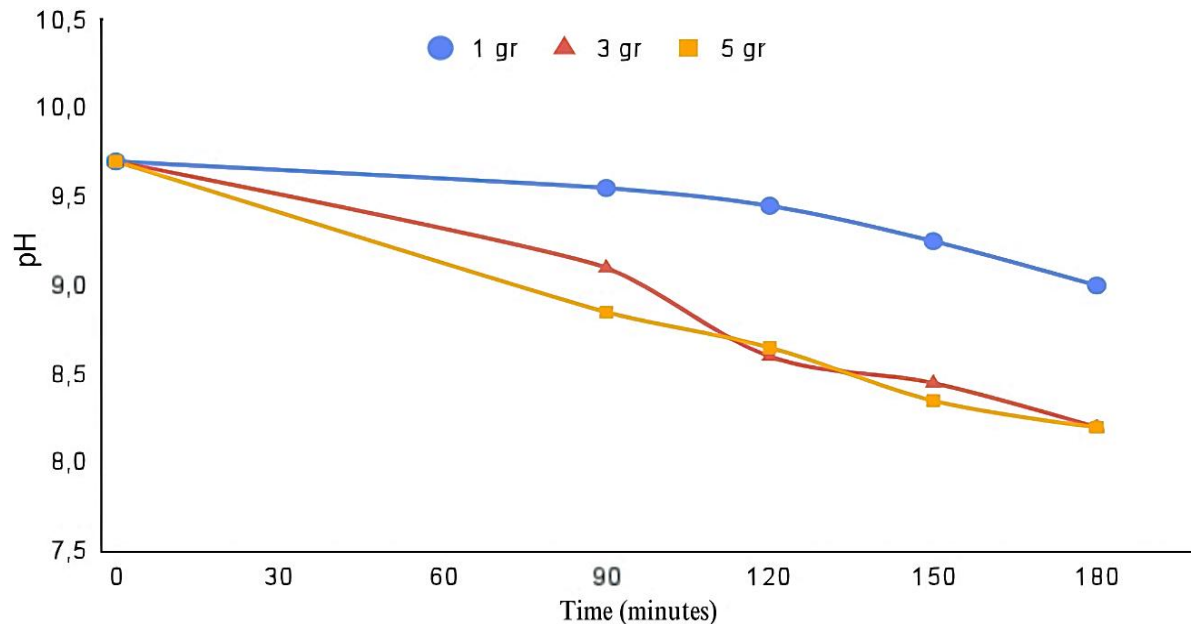


Figure 3 pH value after adsorption process.

The graph on Figure 3 illustrates the change in pH value over time for the three adsorbent mass variations, 1 g, 3 g, and 5 g, during the pH reduction process of laundry wastewater. Initially, the pH value for all variations was 9.7. Over time, pH gradually decreased, with the 3 g and 5 g adsorbents showing greater effectiveness than the 1 g adsorbent. After approximately 160-180 min, the pH values for the 3 g and 5 g adsorbents approached or fell within the standard quality range (6-9) set by PerMen LHK Number 5 of 2014 concerning Wastewater Quality Standards. However, the pH value for the 1 g adsorbent remained above the maximum limit specified by the quality standards. Increasing activated carbon mass accelerates and enhances pH reduction in laundry wastewater. This decrease in pH can occur because activated carbon can adsorb basic compounds in laundry wastewater, thereby reducing the concentration of basic ions in the solution [19]. Increased adsorbent mass provides more active sites for ion uptake, which accelerates the pH reduction process. Longer contact time also allows for optimal interaction between ions and adsorbent, eventually reaching equilibrium [18].

In addition to measuring the pH of the solution, an important factor influencing the interaction between the adsorbent and adsorbate is the zero charge point (pH_{pzc}) of activated carbon. pH_{pzc} refers to the pH at which the adsorbent surface has no net charge. At $pH > pH_{pzc}$, the surface of activated carbon is positively charged, making it easier to attract anions such as phosphate (PO_4^{3-}). Conversely, at $pH < pH_{pzc}$, the surface tends to be negatively charged, resulting in repulsion forces with phosphate anions, which can reduce adsorption efficiency [20] [26]. In this study, the initial pH of laundry wastewater was 9.7, higher than the pH_{pzc} range of biomass-based activated carbon, which is generally 6–7 after H_3PO_4 activation [13]. This explains why phosphate adsorption is optimal only at a certain contact time but decreases after passing the saturation point due to increased electrostatic repulsion and desorption potential. The decrease in solution pH during the adsorption process also indicates a shift towards conditions that better support electrostatic interactions between the activated carbon surface and phosphate ions, thereby improving the effectiveness of phosphate binding.

3.5 Adsorption capacity

Adsorption capacity, typically expressed in mg/g, indicates the amount of a substance adsorbed by an adsorbent under specified conditions. Several factors, including the initial concentration of the adsorbate, pH, temperature, adsorbent surface area, and contact time, influence this capacity. Generally, higher initial concentrations enhance adsorption until saturation is reached. pH, on the other hand, affects the adsorbent's surface

charge and the adsorbate's speciation [20]. This study determined the adsorption capacity using 200 mL of laundry wastewater, with adsorbent masses of 1, 3, and 5 g, contact times of 90, 120, 150, and 180 min, and a stirring speed of 100 rpm.

Table 4 Adsorption capacity.

Adsorbent Mass (g)	Adsorption Time (min)	Initial Concentration (mg/L) (Co)	Final Concentration (mg/L) (Ce)	Volume (L)	Qe (mg/g)
1	90		1.913		0.848
	120		1.896		0.852
	150	6.154	1.832	0.2	0.864
	180		1.252		0.980
3	90		1.328		0.965
	120		1.256		0.980
	150	6.154	1.226	0.2	0.986
	180		1.053		1.020
5	90		0.786		1.074
	120		1.057		1.019
	150	6.154	1.358	0.2	0.959
	180		1.459		0.939

The results of the adsorption capacity, presented in Table 4, show the performance of activated carbon from teak wood powder in removing phosphate from laundry wastewater. At an adsorbent mass of 1 g, the adsorption capacity (Qe) increased with contact time, from 0.848 mg/g at 90 min to 0.980 mg/g at 180 min. Similarly, at an adsorbent mass of 3 g, Qe increased from 0.965 mg/g at 90 min to 1.020 mg/g at 180 min. However, at an adsorbent mass of 5 g, the optimum adsorption capacity occurred at a contact time of 90 min, with a value of 1.074 mg/g. However, it decreased at longer contact times, reaching 0.939 mg/g at 180 min. Overall, Table 4 highlights that the adsorption capacity of activated carbon is influenced by both the adsorbent mass and contact time. Larger adsorbent masses provide more surface area and pores for the adsorption process, but excessive contact times may lead to reduced efficiency, particularly at higher adsorbent masses.

Increasing the mass of teak wood powder-based activated carbon increases the phosphate sorption efficiency due to the availability of active sites and larger pore volume. However, there is an optimal balance between adsorbent mass and contact time that maximizes the adsorption process. For instance, in the study, a carbon mass of 2 g and a contact time of 60 min resulted in the highest phosphate removal efficiency of 80.89%. Beyond the optimal contact time, the adsorption capacity decreased, likely due to desorption, where phosphate ions detached from the saturated adsorbent surface and re-entered the solution [21].

3.6 The effect of adsorbent mass ratio and adsorption time

The first stage in determining the effect of the adsorption process using various variations of mass and contact time on phosphate levels and pH values using multiple linear regression is by conducting several tests, namely the normality test, heteroscedasticity test, multicollinearity test, and autocorrelation test on the data obtained from the study. The normality test results conducted using the Lilliefors Test show that the residual data for the phosphate parameter has a *p*-value of 0.1515. In contrast, the pH parameter has a *p*-value of 0.9037. Since both values exceed the significance level of 0.05, they indicate that the residual data typically follow a normal distribution. Fulfilling this normality assumption is crucial, as it allows for applying the ANOVA method to obtain accurate estimates [22]. Furthermore, the results of the homogeneity test performed using the Bartlett Test show that the variance of the phosphate and pH data is homogeneous, with *p*-values of 0.9788 for both. A *p*-value greater than 0.05 for both parameters indicates no significant difference in variance between the data groups. Thus, we conclude that the classical assumptions of normality and homogeneity support the feasibility of the data for further analysis using the ANOVA test.

Table 5 ANOVA test results.

Parameter	Phosphate			pH			Information
	Df	F Value	P Value	Df	F Value	P Value	
Mass Variation	1	37.832	1.05×10^{-6}	3	346.187	2×10^{-16}	Significant
Time Variation	1	2.800	86.800	3	726	546	Not Significant
Residual	29	-	-	25	-	-	-

Based on ANOVA test (Table 5), the results show that mass variation significantly affects the waste's phosphate levels and pH values. In the phosphate variable, mass variation showed an F value of 37.832 with a *p*-value of 1.05×10^{-6} . Consider mass variation significant if the *p*-value is <0.05 . The significant effect of mass variation indicates that changes in mass directly contribute to changes in the dependent variable [22]. Changes in adsorbent mass significantly impact phosphate levels in the waste and increasing the mass boosts phosphate absorption efficiency.

On the other hand, time variation yielded very low results, with an F value of 0.028 and a *p*-value of 0.868, indicating that treatment time did not significantly affect phosphate levels. For the pH variable, mass variation also showed a significant effect, with an F value of 346.187 and a *p*-value of 2×10^{-16} . Changes in adsorbent mass significantly contribute to changes in the pH value of the waste. However, the effect was adverse, where increasing mass decreased the pH value. Meanwhile, time variation again showed an insignificant effect on pH, with an F value of 0.726 and a *p*-value of 0.546. The significance of these factors was determined through Df, Sum Sq, Mean Sq, F Value, and P Value to ensure the accuracy and validity of the regression model applied [23]. Overall, these results indicate that, among the two factors tested, only mass variation contributes significantly to changes in both phosphate and pH levels. In contrast, time variation does not significantly affect the model. In conclusion, researchers should consider adsorbent mass as a crucial parameter to reduce phosphate levels and control pH in the waste treatment.

3.7 Adsorption Kinetics

Adsorption kinetics describe the rate and mechanism of interaction between the adsorbate and adsorbent. The coefficient of determination (R^2) indicates how much the independent variable influences the dependent variable [23].

Table 6 Determination value (R^2).

Mass (g)	Reaction Order	R^2 Value	Reaction Constant (k)
0	Order 0	0.754	59
	Order 1	0.746	12
	Order 2	0.738	2
	Order 0	0.698	68
1	Order 1	0.682	44
	Order 2	0.667	28
	Order 0	0.894	29
3	Order 1	0.877	24
	Order 2	0.859	2
	Order 0	0.965	77
5	Order 1	0.943	7
	Order 2	0.911	66

Table 6 presents the R^2 value and reaction constant (k) for various adsorbent masses (1, 3, and 5 g) in the context of reactions with 0th, first, and second-order kinetics. For a 5 g mass, the highest R^2 value is 0.965 in the 0th order, the highest value compared to all the other mass conditions. At higher adsorbent masses, the surface area of the activated carbon becomes abundant, causing the phosphate adsorption process to occur at a relatively constant rate, unaffected by the initial concentration of phosphate in the solution. Additionally, the saturation of the pores of the adsorbent causes a fixed amount of phosphate to adsorb over time, a key characteristic of zero-

order kinetics [24]. The analysis shows that the adsorbent mass of 5 g has the highest R^2 value of 0.9649, with the equation $y = 0.0077x + 0.1199$. The results show that the linear model accurately describes the relationship between time and the final concentration of phosphate levels. At higher adsorbent masses, the adsorption pattern tends to be more regular and with a better level of accuracy. The increase in adsorbent mass also contributes to a higher model accuracy in predicting adsorption patterns, as evidenced by the high R^2 value [25]. An increase in adsorbent mass and surface area leads to more consistent interactions between the adsorbent and phosphate ions. This results in a more regular adsorption pattern, as the phosphate ion absorption process occurs more evenly across the adsorbent surface [26].

4. Conclusions

Activated carbon made from teak wood dust has been proven effective in reducing phosphate levels in laundry wastewater, with the highest removal achieved at an adsorbent mass of 5 g over 90 min, reducing phosphate levels from 6.154 mg/L to 0.786 mg/L. Variations in adsorbent mass significantly affect phosphate removal, as indicated by the results of statistical tests, with a phosphate p -value of 1.05×10^{-6} and a pH p -value of 2×10^{-16} . In contrast, variations in contact time did not show a significant effect, with a phosphate p -value of 0.86772 and a pH p -value of 0.748. Researchers consider a parameter significant if the p -value is <0.05 . Furthermore, based on the kinetic analysis, the phosphate adsorption process by activated carbon from teak wood dust aligns more closely with the zero-order kinetic model, with the highest coefficient of determination (R^2) value of 0.965 and an adsorption rate constant (k) of 77 at an adsorbent mass of 5 g.

5. Author contributions

Alfarizi, GA.: Conceptualization, Formal analysis, Investigation, Methodology, Writing – original draft; Pramitasari, N.: Supervision, Validation, Writing – review & editing; Badriani, RE.: Supervision.

6. References

- [1] Haryanto A, Hidayat W, Hasanudin U, Iryani DA, Kim S, Lee S, Yoo J. Valorization of Indonesian wood wastes through pyrolysis: A review. *Energies*. 2021;14(5):1407.
- [2] Islam TU, Abbas E. Validity of ANOVA under non-normality & heterogeneity. *Res Square*. 2022;10:21203.
- [3] Putri DP, Wahida SA, Marlinda. Utilization of epok anana peel (*Musa Paradisiaca* L.) as an adsorbent to reduce COD (*Chemical Oxygen Demand*) levels in laundry wastewater. *J Inform Sains Teknol*. 2022;5:71-77.
- [4] York E, Tadio J, Antwin SO. Simulating studies on phosphate (PO_4^{3-}) removal from laundry wastewater using biochar: Dudinin approach. *Univ J Green Chem*. 2024;2(1):134-136.
- [5] Barambu NU, Peter D, Yusoff MHM, Bilad MR, Shamsuddin N, Marbelia L, Nordin NAH, Jaafar J. Detergent and water recovery from laundry wastewater using tilted panel membrane filtration system. *Membranes*. 2020;10(10):1-9.
- [6] Pramitasari N, Ramadani FB, Azis RA, Bezariani CS, Berliana RI, Badriani RE, Kartini AM, Fildzah CA. Activation of sugarcane bagasse biosorbent with potassium hydroxide and hydrogen chloride to reduce color of batik wastewater. *J Chem Eng Environ*. 2024;19(2):191–199.
- [7] Ibrahim A, Ismail A, Juahir H, Ihsan YN, Sudianto S, Ovinis M, Kassim AM, Hanapi NHM, Hafizi AD. Preparation and characterization of activated carbon obtained from *Melaleuca cajuputi* leaves. *Carbon Trends*. 2023;13:100341.
- [8] Kunusa WR, Iyabu H, Abdullah R. FTIR, SEM and XRD analysis of activated carbon from sago wastes using acid modification. *J Phys Conf Ser*. 2021;1968(1):012034.
- [9] Yusop MFM, Aziz A, Ahmad MA. Conversion of teak wood waste into microwave-irradiated activated carbon for cationic methylene blue dye removal: Optimization and batch studies. *Arab J Chem*. 2022;15(9):103649.
- [10] Herlambang MJ, Ramandani AA, Cendekia D, Alvita LR, Wulandari YR, Shintawati S, Purnani MS, Efendi DAMN. Optimization and characterization of adsorbent from palm kernel shell waste using H_3PO_4 activator. *CHEESA Chem Eng Res Artic*. 2023;6(2):118-120.
- [11] Eso R, Luvi, Ririn. Effect of variation in concentration of activator H_3PO_4 on surface morphology and functional groups of candlenut shell activated Carbon. *Gravit*. 2021;20(1):19–23.

- [12] Tiwow VA, Rampe MJ, Rampe HL, Apita A. Infrared pattern of coconut shell charcoal purified using acid. *Chem Progr.* 2021;14(2):116-119.
- [13] Dittmann D, Saal L, Zietzschatmann F, Mai M, Altmann K, Sabbagh DA, Schumann P, Ruhl AS, Jekel M, Braun U. Characterization of activated carbons for water treatment using TGA-FTIR for analysis of oxygen-containing functional groups. *Appl Water Sci.* 2022;12(8):1-13.
- [14] Fauzia E A, Purnama H. The effect of particle size on the characterization of activated Carbon from tropical black bamboo (*Gigantochloa atroviolacea*). *J Phys Sci Res.* 2021;22(2):99–106.
- [15] Bumajdad A, Hasila P. Surface modification of date palm activated carbonaceous materials for heavy metal removal and CO₂ adsorption. *Arab J Chem.* 2023;16(1):103450.
- [16] Yasdi, Ussarvi D, Rinald, Anggraini FJ, Cahyani SE. Coconut shell-based activated carbon preparation and its adsorption efficacy in reducing BOD from The real wastewater from kitchen restaurant (RWKR): Characteristics, sorption capacity, and isotherm model. *J Presipitasi Komun Pengemb Tek Lingkung.* 2021;18(1):116–130.
- [17] Wahyuhadi ME, Kusumadewi RA, Hadisoebroto R. Effect of contact time on the adsorption process of activated Carbon from banana peel in reducing heavy metal Cd and dyes using a stirring tub (*Pilot Scale*). *IOP Conf Ser Earth Environ Sci.* 2023;1203(1):012034.
- [18] Sutapa JPG, Lukmandaru G, Sunarta S, Pujiarti R, Irawati D, Arisandi R, Dwiyanna R, Priyambodo RD. Utilization of sapwood waste of fast-growing teak in activated carbon production and its adsorption properties. *J Korean Wood Sci Technol.* 2024;52(2):118–133.
- [19] Pungut P, Al Kholif M, Pratiwi WDI. Reduction of chemical Oxygen demand (COD) and phosphate levels in laundry waste using the adsorption method. *J Sains Teknol Lingkung.* 2021;13(2):155-165.
- [20] Ozcan DO, Hendekci MC, Ovez B. Enhancing the adsorption capacity of organic and inorganic pollutants onto impregnated olive stone derived activated Carbon. *Heliyon.* 2024;10(12):e27890.
- [21] Joubory TGH, Hyali EAS, Hadeethi MR. Study of the factors affecting the adsorption efficiency of some chemical pesticides activated carbon at the nanoscale. *Int J Adv Chem Res.* 2023;5(1):89–98.
- [22] Hutami AT, Warsito EA. The effect of fermentation time and mass variation of *Saccharomyces cerevisiae* on the characteristics of virgin coconut oil from the fermentation process of coconut milk. *J Edu Health.* 2023;14(4):801–805.
- [23] Islam MS, Ahmed A, Rahman MM, Hasan MN. Production of activated carbon from sawdust for phosphate removal from wastewater. *J Water Process Eng.* 2023;56:104074.
- [24] Revellame ED, Fortela DL, Sharp W, Hernandez R, Zappi ME. Adsorption kinetic modeling using pseudo-first order and pseudo-second order rate laws: A review. *Clean Eng Technol.* 2020;1:100032.
- [25] Maslukah L, Zainuri M, Wirasatriya A, Widiaratih R. Study of adsorption and desorption kinetics of phosphate ions (PO₄³⁻) in sediments of Semarang and Jepara waters. *J Ilmu Teknol Kelaut Trop.* 2020; 12(2):385–396.
- [26] Hou L, Liang Q, Wang F. Mechanisms that control the adsorption–desorption behavior of phosphate on magnetite nanoparticles: The role of particle size and surface chemistry characteristics. *RSC Adv.* 2020;10(4):2378–2388..
- [27] Zhang L, Liu Z, Cui GL, Chen L. Biomass-derived materials for electrochemical energy storages. *Prog Polym Sci.* 2015;43:136-164.
- [28] Faisal M, Suhartana S, Pardoyo P. Modified natural zeolite Fe metal as phosphate adsorbent (PO₄³⁻) in wastewater. *J Sci Appl Chem.* 2015;18(3):91–95.
- [29] Coates J. Interpretation of infrared spectra, a practical approach. In R. A. Meyers (Ed.), *Encyclopedia of Analytical Chemistry*. Chichester John Wiley Sons Ltd. 2019;10:10815-10837.
- [30] Bakti AI, Gareso PL. Characterization of active carbon prepared from coconut shells using FTIR, XRD, and SEM techniques. *Biruni Sci J Phys Educ.* 2024;7(1):33–39.
- [31] National Standardization Agency. SNI 06-3730-1995: Specification for activated carbon from coconut shell. Jakarta: BSN. 1995.
- [32] National Standardization Agency. SNI 06-6989.31-2005: Water and wastewater - Part 31: Method of Test for Phosphate (PO₄³⁻) Content by Spectrophotometry. Jakarta: BSN. 2005.